THE JOURNAL OF BIOLOGICAL CHEMISTRY VOL. 283, NO. 44, pp. 30101–30111, October 31, 2008

CDKL5 Expression Is Modulated during Neuronal Development and Its Subcellular Distribution Is Tightly Regulated by the C-terminal Tail*

Received for publication, June 17, 2008, and in revised form, August 6, 2008 Published, JBC Papers in Press, August 13, 2008, DOI 10.1074/jbc.M804613200

Laura Rusconi[‡], Lisa Salvatoni[§], Laura Giudici[‡], Ilaria Bertani[‡], Charlotte Kilstrup-Nielsen[‡], Vania Broccoli[§1], and Nicoletta Landsberger[‡1,2]

From the [‡]Department of Structural and Functional Biology, University of Insubria, Via Alberto da Giussano 12, 21052 Busto Arsizio (VA), Italy and the [§]Stem Cell Research Institute, San Raffaele Scientific Institute, 20132 Milan, Italy

Mutations in the human X-linked cyclin-dependent kinase-like 5 (*CDKL5*) gene have been identified in patients with Rett syndrome (RTT), West syndrome, and X-linked infantile spasms, sharing the common feature of mental retardation and early seizures. CDKL5 is a rather uncharacterized kinase, but its involvement in RTT seems to be explained by the fact that it works upstream of MeCP2, the main cause of Rett syndrome. To understand the role of this kinase for nervous system functions and to address if molecular mechanisms are involved in regulating its distribution and activity, we studied the ontogeny of CDKL5 expression in developing mouse brains by immunostaining and Western blotting. The expression profile of CDKL5 was compared with that of MeCP2. The two proteins share a general expression profile in the adult mouse brain, but CDKL5 levels appear to be highly modulated at the regional level. Its expression is strongly induced in early postnatal stages, and in the adult brain CDKL5 is present in mature neurons, but not in astroglia. Interestingly, the presence of CDKL5 in the cell nucleus varies at the regional level of the adult brain and is developmentally regulated. CDKL5 shuttles between the cytoplasm and the nucleus and the C-terminal tail is involved in localizing the protein to the cytoplasm in a mechanism depending on active nuclear export. Accordingly, Rett derivatives containing disease-causing truncations of the C terminus are constitutively nuclear, suggesting that they might act as gain of function mutations in this cellular compartment.

Rett syndrome (RTT,[3] OMIM 312750) is an X-linked neurodevelopmental disorder that occurs almost exclusively in girls with an incidence of 1:10,000 female births. Patients affected with classic RTT are usually born healthy and start manifesting symptoms after an apparently normal period of development lasting 6–18 months (1, 2). Then a rapid regression causes the loss of speech and purposeful movements and the appearance of autistic traits, ataxia, seizures, scoliosis, respiratory crisis, and characteristic stereotypic hand movements. Furthermore, decelerated head growth is typically present, leading to microcephaly within the second year (3). Despite the reduced brain volume, no diminution in neuronal number has been observed, but rather a decrease in cell soma size and dendritic arborization. Approximately 25% of RTT patients are characterized by a clinical picture that does not completely meet the accepted diagnostic criteria; accordingly, several RTT variant forms have been described differing in disease onset and severity (4).

Defects in the methyl-CpG-binding protein 2 (MECP2) and cyclin-dependent kinase-like 5 (CDKL5) genes, located on Xq28 and Xp22, respectively, have been identified as genetic causes of RTT (5–11). Mutations in MECP2 account for more than 95% of patients with classic RTT but have been found in only 20–40% of atypic RTT patients (12). CDKL5 defects have been found in some patients with the Hanefeld variant, a congenital form of RTT characterized by the presence of intractable seizures during the first months of life (7–11, 13). Moreover, mutations or chromosomal translocations involving CDKL5 have also been identified in patients with infantile spasms associated with mental retardation and in West syndrome patients (14–16).

MeCP2 is a transcriptional repressor that binds methylated CpGs in the mammalian genome and silences gene expression through the recruitment of corepressor complexes containing different chromatin modifying activities (17–19). The current model explaining RTT onset in patients with MECP2 mutations suggests that defects occur in the nervous system due to the deregulation of a number of neuronal genes (20). Accordingly, among other genes, MeCP2 has been shown to regulate the expression of the brain-derived neurotrophic factor (*Bdnf*) gene in an activity-dependent manner regulated by the specific phosphorylation of the methyl-binding protein (21–23). However, since the efforts to identify MeCP2 target genes have not been able to justify the dramatic phenotype associated with the lack of the methyl-binding protein, some authors have proposed that MeCP2 functions other than transcriptional repression might play a role in RTT. Accordingly, it has been demon-

* This work was supported by the Rett Syndrome Research Foundation (to C. K.-N. and V. B.), Telethon (to N. L.), Ministero dell'Istruzione dell'Università e della Ricerca (to N. L.), Fondazione Cariplo (to C. K.-N. and N. L.), and the E-rare EuroRETT network (to V. B., C. K.-N., and N. L.). The costs of publication of this article were defrayed in part by the payment of page charges. This article must therefore be hereby marked "*advertisement*" in accordance with 18 U.S.C. Section 1734 solely to indicate this fact.

[1] Both authors contributed equally to this work.

[2] To whom correspondence should be addressed: University of Insubria, Via Alberto da Giussano 12, 21052 Busto Arsizio (VA), Italy. Tel.: 39-0331-339-406; Fax: 39-0331-339-459; E-mail: landsben@uninsubria.it.

[3] The abbreviations used are: RTT, Rett syndrome; CDKL5, cyclin-dependent kinase-like 5; MeCP2, methyl CpG-binding protein 2; GFAP, glial fibrillary acidic protein; NeuN, neuronal nuclei; GABA, γ-aminobutyric acid; MAP2, microtubule-associated protein; LMB, leptomycin B; GFP, green fluorescent protein; NES, nuclear export signal; NLS, nuclear localization signal; GAPDH, glyceraldehyde-3-phosphate dehydrogenase; PBS, phosphate-buffered saline; DAPI, 4′,6-diamidino-2-phenylindole; DMEM, Dulbecco's modified Eagle's medium.

strated that MeCP2 is also involved in regulation of splicing and that aberrant alternative splicing patterns are observed in a mouse model of Rett syndrome (24). Furthermore, the large-scale mapping of neuronal MeCP2 sites has revealed the presence of MeCP2 on a large number of active promoters, an observation, which has recently been reinforced by Ishibashi *et al.* (25, 26). Eventually, very lately it has been proposed that MeCP2 not only works as a repressor but also as an activator of transcription and that, at least in the hypothalamus, the activating functions are predominant (27).

The human CDKL5 gene encodes a protein of 1030 amino acids with an N-terminal catalytic domain highly homologous to members of the mitogen-activated protein (MAP) kinase and cyclin-dependent (CDK) kinase families (28). The protein is rather uncharacterized but its involvement in RTT has been explained by the fact that this kinase seems to function in a molecular pathway common to that of MeCP2 (11, 29). In fact, the two proteins form a protein complex *in vivo* and the catalytic activity of CDKL5 mediates the phosphorylation of MeCP2 *in vitro*. Moreover, the two genes share temporal and spatial expression patterns in the brain and are simultaneously activated during neuronal maturation (11). According to the current model, CDKL5 works upstream of MeCP2 influencing directly or indirectly its phosphorylation state and thereby specific functions of the methyl-binding protein. In the absence of CDKL5, these phosphorylation-dependent activities of MeCP2 would be altered causing a subset of Rett symptoms. In addition, other as yet non-discovered targets of the kinase would also be deregulated, leading to the specific phenotype associated with CDKL5 mutations. In agreement with this model, so far, RTT causing mutations in CDKL5 have been found only in patients with the Hanefeld variant and never associated with classic RTT. The fact that the autonomous nervous system, whose malfunction in patients with MECP2 mutations causes severe respiratory problems and constipation, appears to be better preserved in patients with CDKL5 deficits reinforces also separate functions of the two proteins (30).

Whereas substantial information has been gathered regarding the expression and localization of the MeCP2 protein in the nervous system, CDKL5 remains completely uncharacterized. MeCP2 is expressed in the embryonic brain but its levels increase significantly during late embryonic stages reaching levels that remain rather uniform during postnatal development where the methyl-binding protein is found in the nucleus of most neurons of the adult brain (31–35). The induction of MeCP2 expression follows that of neuronal maturation, and the precise protein levels have shown to be crucial for correct synapse formation (23).

To better understand the role of CDKL5 in the nervous system and to understand when and where it might enter in contact with the methyl-binding protein, we have analyzed in detail the expression profile of this kinase in embryonic and postnatal brains from normal mice and compared it to that of MeCP2. Our data demonstrate that despite an expression profile generally overlapping that of MeCP2, CDKL5 peaks later in development, and its levels appear to be much more modulated than those of MeCP2. Furthermore, whereas MeCP2 is an exclusively nuclear protein, CDKL5 shuttles between the two main cellular compartments and the relative concentrations in each compartment seem to vary in different brain areas and during development. Eventually, we demonstrate that the C-terminal region of CDKL5, which is frequently deleted in pathogenic mutations, is involved in an active nuclear export mechanism modulating the subcellular distribution of the kinase.

EXPERIMENTAL PROCEDURES

Cell Cultures—Astroglial cell cultures were prepared from newborn mice. Using a sterile technique, the animals were decapitated, the brains were removed and placed in Petri dishes containing PBS and penicillin-streptomycin. The cortical tissue was separated from the meninges and dissociated by trituration with a Pasteur pipette. Cells were grown in T75 flasks containing DMEM (Invitrogen) supplemented with 10% fetal calf serum and 2 mM glutamine. Cultures were kept at 37 °C in a humidified 5% CO_2 atmosphere. The medium was changed every 3 days. Astroglial cell cultures consisted of >90% glial fibrillary acidic protein-positive cells, ~1% neurons, and ~3% microglial cells.

Primary neuronal cultures were prepared from the cortex of day 17.5 mouse embryos (E17.5). Briefly, cortical cells were dissociated and centrifuged at 800 rpm for 5 min, resuspended in DMEM with 10% horse serum (HS, Invitrogen) by gentle trituration with a Pasteur pipette and plated at 45.000 cells/cm^2 in modified DMEM-HS on poly-D-lysine-coated glass coverslips (Sigma-Aldrich). After 3 h, the medium was replaced with Neurobasal medium containing B27 supplement (Invitrogen) and 2 mM glutamine, and incubated at 37 °C in a humidified incubator with 5% CO_2 for 10 days. Human HeLa cells were maintained in DMEM supplemented with 10% fetal calf serum at 37 °C with 5% CO_2. Leptomycin B treatment was performed with 50 nM LMB for 3 h prior to fixation.

Plasmids—GFP-hCDKL5 was described previously (29); GFP-Δ941 (amino acids 1–941), GFP-Δ831 (amino acids 1–831), GFP-832–1030 (amino acids 832–1030), GFP-L879X (amino acids 1–878), and GFP-R781X (amino acids 1–780) contain the indicated regions of hCDKL5 cloned into the BamHI site of pEGFP-C1 (Clontech). All constructs were generated by PCR and sequence-verified.

Antibodies—A rabbit anti-MeCP2 anti-serum (Covance Research Product Inc.) was raised against hMeCP2 (amino acids 171–486) expressed in *Escherichia coli* as a fusion protein containing a chitin-binding domain that was eliminated during the purification procedure. This antibody was used 1:1000. For some experiments, a polyclonal anti-MeCP2 antibody (Sigma, 1:1000) was used.

Moreover, the following antibodies were used in Western blotting, immunohistochemistry, and/or immunofluorescence experiments: rabbit polyclonal anti-CDKL5 (1:1000 in Western blotting in Figs. 1 and 5; when purified against the antigen spanning amino acids 301–751 the antibody was used 1:50 in Western blotting (Figs. 2, 4, and 6) and 1:5 in immunofluorescence and immunohistochemistry experiments; Covance Research Product Inc.; Ref. 29), mouse monoclonal anti-GABA (1:200, Sigma); mouse monoclonal anti-NeuN (1:100, Chemicon); anti-MAP2 (1:200, Sigma), anti-GAPDH (1:2000, Open BIOSOURCE), and anti-actin (1:5000, Sigma).

Immunohistochemistry—For immunohistochemistry experiments, C57BLJ6 mice were used. Newborn mice (P0), and mice of postnatal stages 12.5 (P12.5), and P120 were anesthetized by intraperitoneal injections of chloral hydrate, and the brains were fixed by intracardiac perfusion with NaCl 0,9%, followed by 4% paraformaldehyde (PFA) in PBS. Brains were removed and postfixed for 4–6 h in 20% sucrose in 4% PFA at 4 °C, placed in 20% sucrose in PBS overnight and frozen in dry ice. Cryostat sections were cut in the saggital or coronal plane at 20 μm and rinsed three times in PBS. Sections were incubated for 1 h at room temperature in 10% goat serum (Sigma) and 0,5% Triton X-100 (Sigma) in PBS, then incubated with the primary antibody overnight at 4°C in the same solution. The next day, sections were rinsed three times and incubated at room temperature for 1 h in a secondary antibody solution of biotinylated goat anti-rabbit IgG (Vector Laboratories, Burlingame, CA) at 1:200 in PBS. After three washes, sections were incubated with the avidin-biotin complex in PBS for 1 h using the Vectastain Elite ABC kit, washed three times and the staining visualized by incubation with 0.5 mg/ml 3,3′-diaminobenzidine tetrahydrochloride (Sigma) and 0.3 μl/ml hydrogen peroxide in PBS. Sections were dehydrated in ascending alcohols and mounted with DPX mounting media. To control for the specificity of the signal, sections were run through the entire procedure but without the incubation with the primary antibodies.

The human brain samples are an autopsy from a postmortem brain and an operatory biopsy, respectively, from two adult women (ages 63 and 21 years old). Five micrometer sections were cut from the formalin-fixed and paraffin-embedded tissue and used for immunohistochemistry experiments following the above procedures.

Immunofluorescence—Human HeLa cells were seeded on gelatin-coated glass coverslips and transiently transfected with Lipofectamine 2000 (Invitrogen). 16-h post-transfection, the cells were fixed with 4% PFA, stained with 4′,6-diamidino-2-phenylindole dihydrochloride (DAPI; Sigma), and the specific GFP signals analyzed with an Olympus BX51 Fluorescence microscope.

For fluorescent double labeling, free-floating brain sections from adult C57BLJ6 mice or primary cortical neurons were stained. After 1 h in blocking solution (PBS, 5% fetal bovine serum, 0.5% Triton X-100), sections were incubated overnight at 4 °C with the primary antibody. Sections were rinsed three times in PBS and incubated with Alexa 555 goat anti-rabbit IgG antibody (1:2000, Molecular Probes) and Alexa 488 goat anti-mouse IgG antibody (1:2000, Molecular Probes) for 1 h at room temperature. After nuclear staining with DAPI for 5 min, they were mounted on glass slides and coverslips were applied using Moviol (Sigma) mounting medium. The slides were analyzed on an Olympus BX51 Fluorescence microscope.

Mouse primary neurons were grown for 10 days *in vitro* and fixed with 4% PFA. After 10 min in permeabilization solution (HEPES 20 mM pH 7.4, sucrose 300 mM, $MgCl_2$ 3 mM, Triton X-100 0.2%) and 15 min in PBS, 5% fetal bovine serum, cells were incubated overnight at 4 °C with primary antibodies in PBS, 5% fetal bovine serum, and 0.2% Triton X-100. Cells were rinsed three times, incubated with secondary antibodies, the nuclei stained with DAPI for 5 min, and the coverslips mounted for microscopy.

Protein Extraction and Western Blotting—Brain tissue fractionation was performed as follows. Differently aged CD1 mice were killed, brains or carefully dissected brain areas were rapidly explanted on ice, and homogenized in cytosolic lysis buffer (HEPES pH 7.5 20 mM; $MgCl_2$ 1.5 mM; KCl 10 mM; dithiothreitol 2 mM) by 50 strokes with an automatic Potter. A protease/phosphatase inhibitor mix (Na_3VO_4 1 mM; phenylmethylsulfonyl fluoride 1 mM; protease inhibitor mixture (Roche Applied Sciences); NaF 1 mM) was used in all the buffers. Homogenates were centrifuged at 2000 × *g* at 4 °C for 5 min, and the supernatant was collected as the cytosolic fraction. The nuclei were washed once with cold PBS, lysed in nuclear lysis buffer (HEPES pH 7.5 20 mM; $MgCl_2$ 1.5 mM; NaCl 420 mM; SDS 1%; EDTA 0,2 mM; glycerol 25%; dithiothreitol 2 mM) and incubated for 30 min at 100 °C. After incubating overnight on a wheel at room temperature, samples were centrifuged at 20,000 × *g* for 30 min. The supernatant was recovered as the nuclear fraction. In parallel, total lysates were prepared homogenizing brain and cerebellar tissues in total lysis buffer (HEPES pH 7.5 20 mM; $MgCl_2$ 1.5 mM; NaCl 420 mM; EDTA 0.2 mM; glycerol 25%; dithiothreitol 2 mM), adding SDS 1% and proceeding as for nuclear lysis. The protein content was dosed by bicinchonic acid assay (Pierce). Samples were conserved in Laemmli buffer and processed by immunoblotting.

For Western blotting, the proteins were separated on 10% SDS-PAGE, transferred to nitrocellulose membranes, and the blots incubated with antibodies against MeCP2, CDKL5, GAPDH, and/or actin. A Kodak Image Station 2000R was used to quantify the signals.

RESULTS

As already mentioned, recent clinical and biochemical data suggest that CDKL5 belongs to the same molecular pathway as MeCP2 (11, 29); however, it remains unknown in which brain area(s) and developmental stages this functional interaction should occur. We therefore performed immunohistochemistry experiments to study the expression profile of CDKL5 in mouse brains and compared it at the regional level to that of MeCP2. As shown in Fig. 1, in the adult mouse brain the two proteins showed very similar expression patterns, which is consistent with the fact that they work in a common molecular pathway. In fact, both CDKL5 and MeCP2 are diffusely expressed in all the brain structures analyzed at adult stages. Both proteins could be detected in the cerebral cortex (Fig. 1, *panels A*, *E*, *I*, and *M*), hippocampus (Fig. 1, *panels B*, *F*, *J*, and *N*), cerebellum (Fig. 1, *panels C*, *G*, *K*, and *O*), and brain stem (Fig. 1, *panels D*, *H*, *L*, and *P*). Therefore, these immunohistochemistry experiments revealed a similar dispersed but consistent expression of both proteins in virtually all cells of the different brain areas. In a parallel approach, by Western blotting on whole cell lysates obtained from carefully dissected brain areas, we compared MeCP2 and CDKL5 protein levels in the different brain districts. The signal corresponding to CDKL5 and MeCP2, respectively, were normalized to GAPDH levels, and the relative amounts illustrated in Fig. 1*R*. As seen in the Western blot (Fig. 1*Q*), MeCP2 levels appear rather uniform among the different areas except the cerebellum where it is highly expressed. CDKL5 levels are, on the other hand, more modulated; in fact,

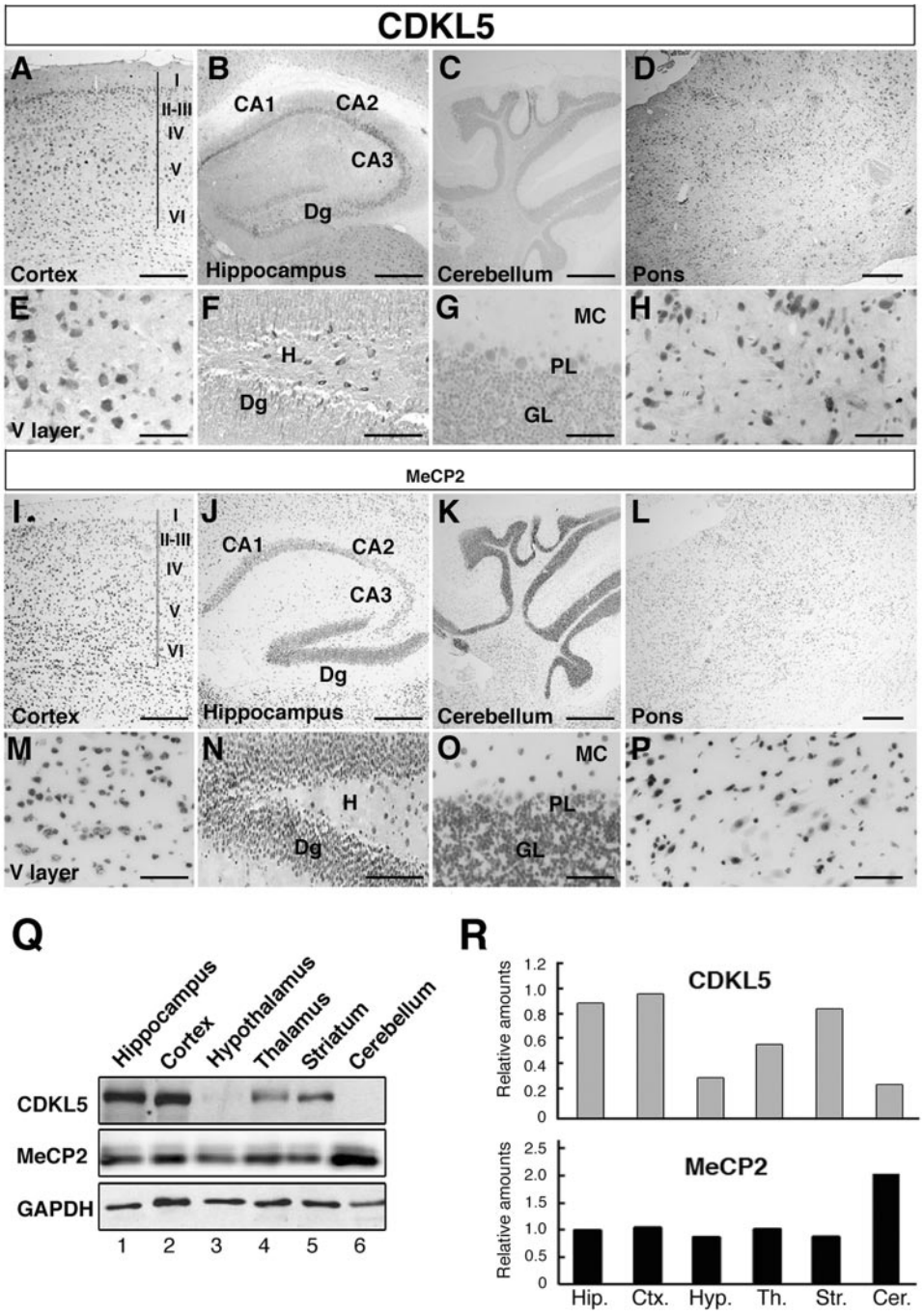

FIGURE 1. **CDKL5 levels vary between the individual brain areas of P120 mice.** *A–P*, immunohistochemistry experiments showing CDKL5 and MeCP2 expression in serial sections of an adult mouse brain (P120). The different panels show: cortex (*A*, *E*, *I*, *M*), hippocampus (*B*, *F*, *J*, *N*), cerebellum (*C*, *G*, *K*, *O*), and pons (*D*, *H*, *L*, *P*) of the adult mouse brain (P120). *Panels E–H* and *M–P* are magnifications of *A–D* and *I–L*, respectively. I-VI (*panels A* and *I*) indicate the different cortical layers; *Dg*, dentate gyrus; *H*, hilus; *GL*, granule cell layer; *PL*, Purkinje cell layer; *MC*, molecular cell layer. *Q,* Western blot showing CDKL5 and MeCP2 protein levels (*upper and middle panels*, respectively) in whole cell lysates prepared from dissected areas of a P120 brain. GAPDH was used as loading control (*lower panel*). *R*, graphic illustration showing the relative CDKL5 and MeCP2 levels (*upper and lower graph*, respectively) in hippocampus (*Hip.*), cortex (*Ctx.*), hypothalamus (*Hyp.*), thalamus (*Th.*), striatum (*Str.*), and cerebellum (*Cer.*) of the P120 mouse brain. CDKL5 and MeCP2 levels in the Western blot (*panel Q*) were normalized to GAPDH setting cortical levels arbitrarily to 1. *Scale bars*: *A*, *I*, *D*, *L* = 300 μm; *B*, *J* = 500 μm; *C*, *K* = 800 μm; *E*, *H*, *M*, *p* = 30 μm; *G*, *O* = 50 μm.

whereas significant amounts of CDKL5 are found in the adult hippocampus, cortex, thalamus, and striatum (Fig. 1*Q*, *lanes 1*, *2*, *4*, and *5*), the levels of the kinase appear more reduced in the hypothalamus and cerebellum (*lanes 3* and *6*). This is in accordance with the immunohistochemistry experiments where CDKL5 appeared less intense but with significant expression in granular (GL) and Purkinje (PL) cells (Fig. 1, *panels C*, *G*, and *K*, *O*).

MeCP2 has been reported to be expressed in late embryonic and early postnatal stages where its profile correlates with neuronal maturation (31, 34). To understand the dynamics of CDKL5 expression, we compared the pattern of the two proteins in the cortex and hippocampus at embryonic day 16.5 (E16.5), newborn (P0), postnatal days 12.5 and 120 (P12.5 and P120, respectively). As reported previously, MeCP2 is expressed rather uniformly in the cortex already at E16.5; in early postnatal stages its expression gets modulated, though, and in adult stages the protein levels are higher in layer V correlating with highest levels in more mature neurons (31, 33, 34). Surprisingly, CDKL5 presented a developmental expression profile very similar to that described for MeCP2. In fact, CDKL5 was only minimally detectable at embryonic stage E16.5 (Fig. 2, *panel A*) while it was induced in maturing neurons residing in the cortical plate (cp) at perinatal stages (Fig. 2, *panel B*). During the following postnatal development, CDKL5 gets strongly up-regulated in both cerebral cortex and hippocampus (Fig. 2, *panels C*, *D*, *F*, and *G*). To summarize, the immunohistochemistry experiments indicate that CDKL5 expression is very low in abundance in the embryonic cortex and is strongly induced in early postnatal stages. To confirm this observation, we performed Western blotting on total brain extracts obtained from mice at different embryonic and postnatal stages. As can be seen in Fig. 2 (*panels O* and *P*), these experiments confirmed that CDKL5 is very low in abundance (but not absent, see Fig. 6, *panel A*) in the brain of mouse E18 embryos and is induced in early postnatal stages. A quantification of the obtained data indicates that, in the brain, CDKL5 is expressed at maximum levels at P14 and then declines slowly up to adult stages (data not shown). In con-

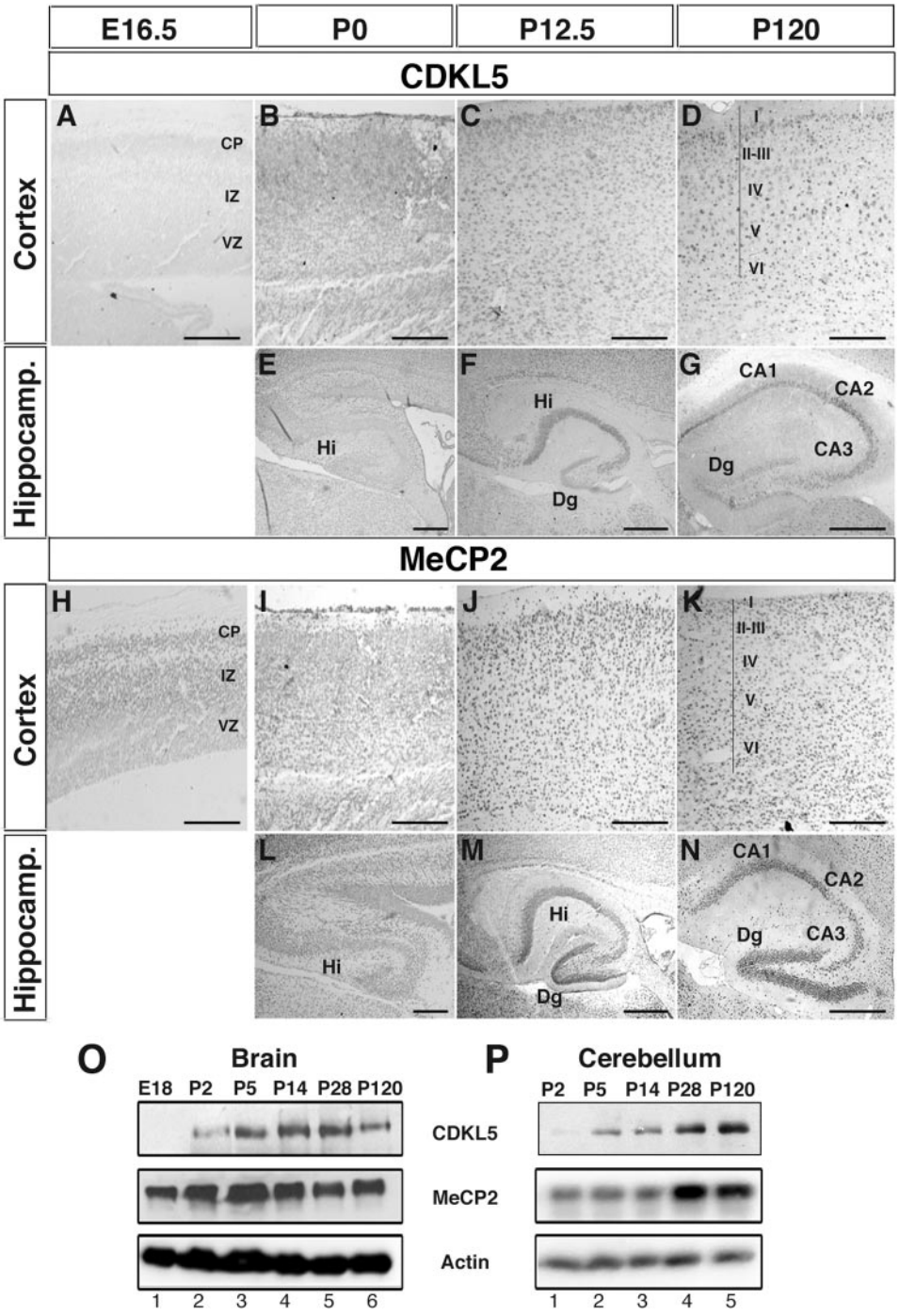

FIGURE 2. **CDKL5 expression is highly induced at early postnatal stages of brain development.** *A–G*, immunohistochemistry experiments showing CDKL5 expression in the cortex (*A–D*) and hippocampus (*E–G*) of mouse brains at the indicated embryonic or postnatal stages. *H–N*, MeCP2 expression in the cortex (*H–K*) and hippocampus (*L--N*) of mouse brains at different developmental stages. *CP*, cortical plate; *IZ*, intermediate zone; *VZ*, ventral zone; *Hi*, hippocampus; *Dg*, dentate gyrus; *I-VI*, different cortical layers. *O* and *P*, Western blot showing CDKL5 and MeCP2 protein levels (*upper and middle panels*, respectively) in total brain (*O*) or cerebellar (*P*) extracts at E18, P2, P5, P14, P28, and P120 stages. Actin was used as loading control (*lower panel*). *Scale bars*: *A–D*, *H–K* = 500 μm; *E–G*, *L–N* = 500 μm.

trast, and in accordance with published results, MeCP2 levels are rather constant from E18 to adult stages. In the cerebellum, the expression of CDKL5 appears to be induced slightly later and continues to increase until adult stages. Concerning MeCP2, we observed a significant increase during late postnatal development.

Because CDKL5 deficiency has a strong impact on human brain functions, we wondered how the protein was localized in human adult brain tissues. Immunohistochemistry experiments revealed numerous and diffusely CDKL5-positive cells in both the cerebral cortex and corpus callosum with a general pattern very similar to that observed in the adult mouse brain (Fig. 3, *panels A–D*). Furthermore, in the human cerebellum, CDKL5 was detected in the majority of the cells corresponding to granular, molecular, and Purkinje cell layers, although increased levels were present in Purkinje neurons in agreement with what was described above in the murine cerebellum.

Even though MeCP2 has always been reported to be a neuron-specific protein, an MeCP2-enhanced green fluorescent protein reporter mouse line obtained by knocking in the EGFP cDNA in the Mecp2 locus has recently permitted to demonstrate the presence of MeCP2, at low levels, in differentiated GFAP-positive cells (36). We therefore decided to exploit immunofluorescence and Western blotting assays to address which cells express CDKL5. Fig. 4, *panels A–C* and *E*, clearly demonstrate that virtually all NeuN-positive neurons express CDKL5; in contrast, we were unable to detect CDKL5 in GFAP-positive cells (data not shown). Accordingly, a Western blotting assay performed on a whole cell extract prepared from cultured primary astrocytes did not reveal any CDKL5 expression (Fig. 4, *panel D*), suggesting that the kinase is virtually absent or of very low abundance in the glia.

The above experiments show that CDKL5 is expressed in the majority of the neuronal fraction regardless the neural origin taken into analysis. It appears however, that some neurons display increased levels of CDKL5. In particular, in the dentate gyrus, GABAergic cortical interneurons within the hilus express CDKL5 much stronger than the dentate granular neurons (Fig. 4, *panels F–H*). Similarly, in the cerebellum, Purkinje cells express significantly more CDKL5 than the granular or stellate cells (*panels L–N*). These results indicate that CDKL5 levels are finely tuned in

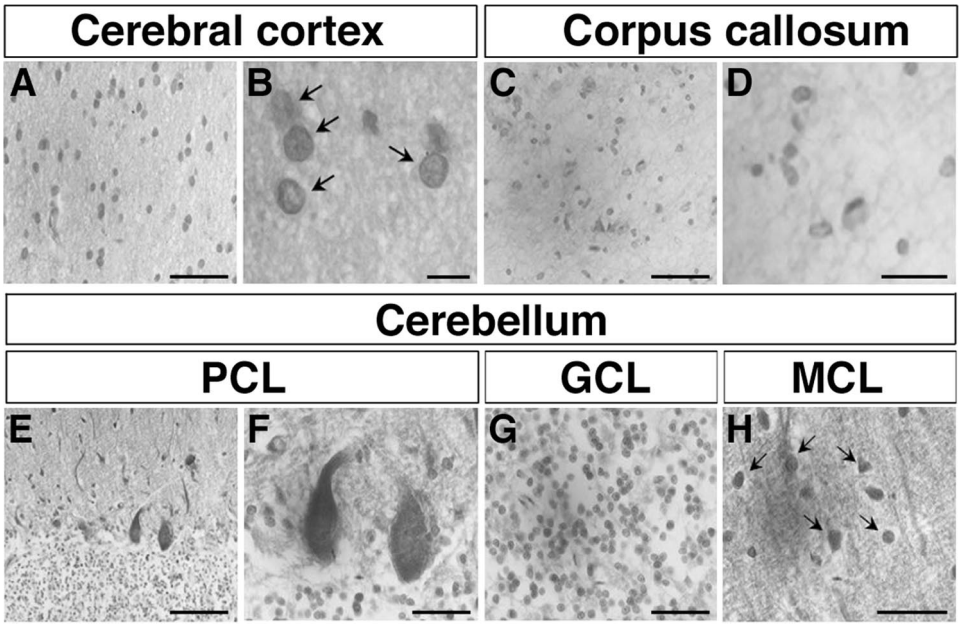

FIGURE 3. **CDKL5 has a diffuse expression in most cells of the adult human brain.** Immunohistochemistry experiments showing CDKL5 expression in cerebral cortex (*A* and *B*), corpus callosum (*C* and *D*), and cerebellum (*E–H*) of adult human brain. *Arrows* indicate some CDKL5-positive cells. *PCL*, Purkinje cell layer; *GCL*, granule cell layer; *MCL*, molecular cell layer. *Scale bars*: *A*, *C*, *E*, *G* = 30 μm; *B*, *F* = 10 μm; *D*, *H* = 20 μm.

different neuronal populations, suggesting that a strict control of CDKL5 levels is required to regulate specific neuronal activities. In accordance with these results, we also observe that even if CDKL5 is present in both glutamatergic and GABAergic primary cultured neurons, the expression levels are highest in the latter cell population (data not shown).

Eventually, immunofluorescence experiments were used to analyze the distribution of endogenous CDKL5 in cultured primary cortical neurons. As indicated in Fig. 4, *panels R–T*, a significant part of endogenous CDKL5 is present in the nucleus where it shows a typical dotted staining; interestingly a significant fraction of CDKL5 is localized in the dendrites.

In the above experiments it emerges that endogenous CDKL5 is significantly expressed in both nucleus and cytoplasm of cultured cortical neurons and in different neurons throughout the brain. Therefore, we decided to analyze whether the subcellular distribution of the protein might be regulated and vary during development. Cytoplasmic and nuclear extracts were prepared from different brain areas and analyzed by Western blotting using GAPDH and MeCP2 as markers of the cytoplasmic and nuclear fractions, respectively. As shown in Fig. 5*A*, and illustrated graphically in Fig. 5*B*, an almost equal distribution of CDKL5 between cytoplasm and nucleus is found only in some regions; in fact, in the hippocampus, cortex, hypothalamus, and thalamus, ~40% of the protein is nuclear. Conversely, in the striatum and cerebellum the cytoplasmic fraction accounts for almost 80% of CDKL5. These results show that not only do the total levels of CDKL5 vary between different brain areas but, importantly, also that the specific distribution of the protein between the two main cellular compartments differs. To investigate whether the subcellular distribution of CDKL5 is regulated also during development we analyzed by Western blotting cytosolic and nuclear extracts from whole brains at different developmental stages using actin as a loading control. In the Western blot in Fig. 6*A* and the graphic illustration in Fig. 6*B*, it appears that CDKL5 in late embryonic and early postnatal stages is predominantly cytoplasmic with less than 20% of the protein being present in the nucleus (*lanes 7–9*). In P14 brains, however, the nuclear fraction increases to ~40% and remains as such until adult stages (*lanes 10–12*). This dynamic distribution of CDKL5 is opposed to that of MeCP2, which appears to be predominantly nuclear at all developmental stages with a small cytoplasmic fraction in late embryonic and the earliest postnatal stages. Summarizing the obtained data, we suggest that whereas MeCP2 exerts its functions mainly, if not exclusively, in the cell nucleus, the subcellular distribution of CDKL5 depends on the physiological state of the cell.

The above results clearly indicate that regulatory mechanisms modulate the subcellular localization of CDKL5 in murine brain development. Active nuclear export mechanisms depending on nuclear export receptors are responsible for driving many nuclear proteins to the cytoplasm. Nuclear export mediated by the receptor CRM1/Exportin 1 is sensitive to the drug leptomycin B (LMB; 37); to test whether CDKL5 might be actively exported from the nucleus through a CRM1-dependent pathway we analyzed the subcellular localization of hCDKL5 fused to GFP (GFP-CDKL5) in human HeLa cells treated or not with LMB. As shown in Fig. 7*A*, GFP-CDKL5 is found in both the nucleus and cytoplasm in the majority of untreated HeLa cells even if the overall situation is rather heterogenous with some cells expressing the protein solely in the nucleus or cytoplasm, respectively; on the other hand, we observed that after 3 h of treatment with 50 nM LMB, the majority of the protein had accumulated in the nucleus (Fig. 7*A*, *panels a* and *b*, respectively). Interestingly, CDKL5 has a distinct dotted staining in the nucleus as well as in the cytoplasm; the nature of these dots will be revealed by future experiments. The pan-cellular localization of GFP alone was not sensitive to LMB whereas a GFP fusion protein, used as positive control, containing *bona fide* nuclear export and import signals accumulated significantly in the nucleus of LMB-treated cells (data not shown). To map the region within CDKL5 involved in this LMB-sensitive cytoplasmic localization, we tested the subcellular localization of two derivatives of the kinase progressively deleted in the C-terminal region as illustrated graphically in Fig. 7*C*. Whereas the deletion of the region spanning amino acids 942–1030 (GFP-Δ941) did not influence the localization of the fusion protein, a CDKL5 derivative lacking the most C-terminal 200 amino acids (GFP-Δ831) was confined to the cell nucleus, demonstrating that a signal for LMB sensitive cytoplasmic localization of CDKL5 is present in this region (Fig. 7*A*, *panels c*

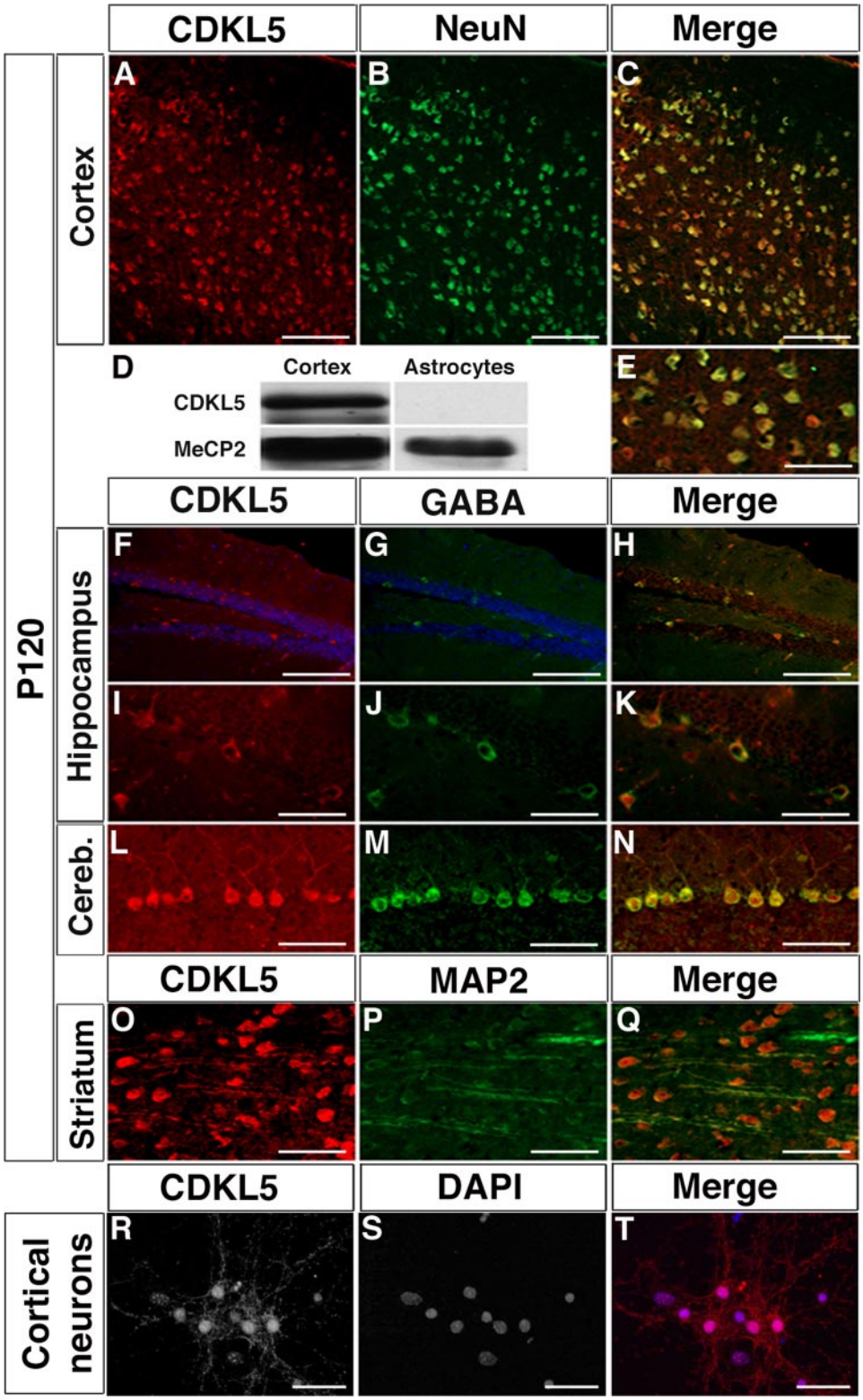

FIGURE 4. **CDKL5 is a pan-neuronal protein in the adult mouse brain.** *A–C* and *E*, Immunofluorescence experiments showing CDKL5 expression in cortical NeuN-positive neurons of a P120 mouse brain; *D*, Western blot showing CDKL5 and MeCP2 expression in whole cell extracts of cultured primary cortical neurons and astrocytes; *F–N*, CDKL5 expression in hippocampus (*F–K*) and cerebellum (*L–N*) is particularly high in GABAergic neurons (*G*, *J*, *M*); *O–Q*, CDKL5 colocalizes with MAP2-positive dendrites of neurons within the striatum. *Panel E* is a magnification of *panel C*. *Panels C*, *E*, *H*, *K*, *N*, and *Q* are merged images of CDKL5 (*A*, *F*, *I*, *L*, and *O*) and NeuN (*B*), GABA (*G*, *J*, *M*), and MAP2 (*P*), respectively. *R* and *S*, immunofluorescence of endogenous CDKL5 in primary cortical neurons (*R*; 10DIV). DAPI staining is shown in *panel S* and the merge in *panel T*. *Scale bars*: *A–C*, *F–H* = 150 μm; *E*, *I–Q* = 30 μm; *R–T* = 40 μm.

and *e*, respectively). When the very C-terminal tail spanning amino acids 832–1030 of CDKL5 was fused to GFP (GFP-832–1030) we observed that the chimeric protein was excluded from the nucleus and that the addition of LMB to the cells did not cause a nuclear accumulation of the protein (Fig. 7*A*, *panels g* and *h*, respectively). We suppose that the fusion protein cannot enter the nucleus due to the absence of a signal for nuclear import and its size of ~52 kDa, probably rendering it too big for passing the nuclear membrane by passive diffusion. In accordance with CDKL5 being able to enter the nucleus, the ScanProsite program identifies two putative nuclear localization signals positioned at 312–315 and 784–789, respectively, both missing in this construct. The signal located between amino acids 784–789 proved to be sufficient for localizing GFP to the cell nucleus (data not shown), and we believe that the nuclear localization of GFP-Δ781 (see below) is due to the presence of the more N-terminal signal at 312–315.

CRM1-mediated nuclear export depends on export signals (NES) within the substrates (37). An inspection of the primary structure of CDKL5 revealed the presence of a stretch of amino acids from 836 to 845 (LKSLRKLLHL) sharing high homology with the consensus NES ($LX_{(2,3)}$[LIVFM]$X_{(2,3)}LX$[LI]; 38). To test whether the putative NES *per se* might be able to direct nuclear export of a heterologous protein, we fused the region containing amino acids 832–879 to GFP (GFP-(832–879)) and expressed the protein in HeLa cells. In this case, however, we observed a similar pan-cellular distribution of both GFP and GFP-(832–879) (data not shown). Furthermore, the substitution of three leucines with alanines, which is normally sufficient to inhibit the activity of a functional NES, did not alter the subcellular localization of GFP-CDKL5 (data not shown). These results indicate that the leucine-rich sequence within the C-terminal tail

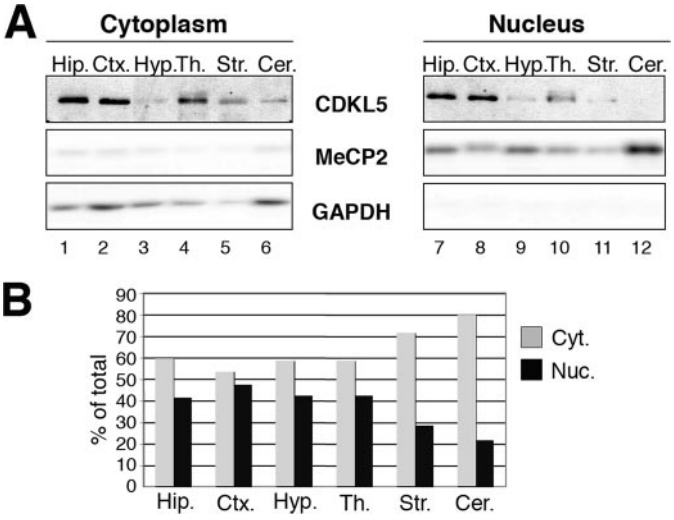

FIGURE 5. **The subcellular distribution of CDKL5 varies between the individual areas of the adult mouse brain.** *A*, fractionated cytoplasmic and nuclear extracts were prepared from carefully dissected brain areas of P120 mice and CDKL5 levels determined by Western blotting using MeCP2 and GAPDH as nuclear and cytoplasmic markers (*upper*, *middle*, and *lower panels*, respectively). *B*, graphic illustration showing the relative levels of cytoplasmic and nuclear CDKL5 (*gray* and *black bars*, respectively) in the different brain areas. *Hip.*, hippocampus; *Ctx*, cortex; *Hyp.*, hypothalamus; *Th.*, thalamus; *Str.*, striatum; *Cer.*, cerebellum. The band intensities in *A* were quantified using a KODAK Image Station 2000R and the sum of cytoplasmic and nuclear CDKL5 set arbitrarily to 100%.

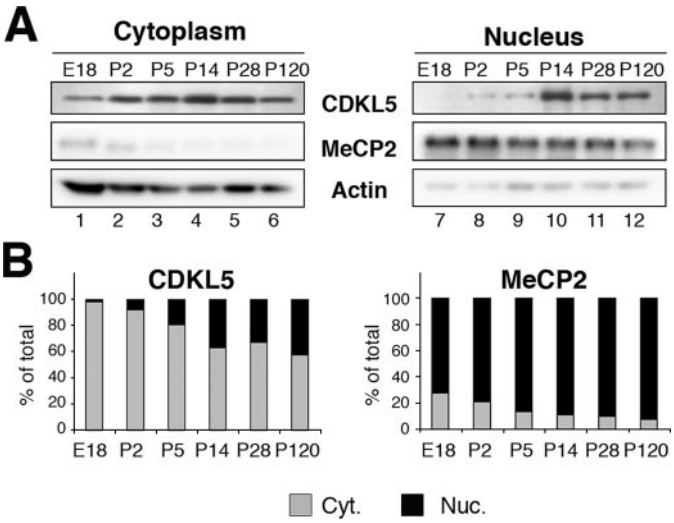

FIGURE 6. **The nuclear localization of CDKL5 is induced at early postnatal stages of the developing mouse brain.** *A*, fractionated cytoplasmic and nuclear extracts were prepared from total brains of E18, P2, P5, P14, P28, and P120 mice and relative levels of CDKL5 and MeCP2 analyzed by Western blotting (*upper* and *middle panels*, respectively). Actin was used as loading control (*lower panels*). *B*, graphic illustration showing the relative cytoplasmic and nuclear levels (*gray* and *black bars*, respectively) of CDKL5 (*left*) and MeCP2 (*right*). The band intensities in *A* were quantified with a KODAK Image Station 2000R and the sum of cytoplasmic and nuclear fractions set arbitrarily to 100%.

of CDKL5 might not be sufficient to be recognized by the nuclear export receptors and that the LMB-sensitive cytoplasmic localization of the kinase is due to an indirect mechanism.

Our data therefore suggest that the subcellular distribution of CDKL5 is modulated through active import and export mechanisms and that the long C-terminal tail is the domain mainly involved in this regulation. However, our previous publication suggested that the nucleo-cytoplasmic distribution of CDKL5 depends also on its catalytic activity; these results have been confirmed using the kinase-dead K42R derivative that, compared with the wild-type protein, is characterized by a negligible nuclear fraction (Ref. 29 and data not shown).

Eventually, considering that several pathological truncations occur in the C-terminal region of CDKL5, we reasoned that some of them might alter its subcellular localization. We therefore analyzed the subcellular localization of two RTT CDKL5 derivatives deleted within the C-terminal region (L879X and R781X), respectively, containing or not the putative NES. When these two derivatives, fused to GFP, were overexpressed in human HeLa cells we observed a nuclear localization of both fusion proteins (Fig. 7*B*). These data reinforce the role of the very C-terminal region in localizing the wild-type protein to the cytoplasm; furthermore, in accordance with the above data, they demonstrate that the leucine-rich NES-like signal spanning amino acids 836–845 and present in the L879X derivative is not solely responsible for localizing CDKL5 to the cytoplasm.

DISCUSSION

During the last few years, mutations in the X-linked *CDKL5* gene have been identified in a number of patients with severe encephalopathy and early onset of epilepsy. To date, disease causing mutations have been identified in 29 patients with X-linked infantile spasms, atypical Rett syndrome, and infantile spasms (7–11, 14–16). The common feature describing these patients is the appearance of epilepsy during the very first weeks of life and a developmental delay without any period of normal development; in many cases the epilepsy becomes refractory to treatment during later stages (39). The majority of mutations have been identified in the so-called Hanefeld variant of RTT, which as opposed to classic RTT has never been associated with mutations in MECP2 (7–11). In accordance with the above description, the occurrence of early seizures characterizes the Hanefeld variant; moreover, the absence of respiratory problems and constipation in many patients with this RTT variant indicates a better preservation of the autonomous nervous system in patients with CDKL5 mutations as compared with those with loss of MeCP2 functions (30).

Even if the above data clearly indicate an important role of CDKL5 for nervous system functions, the protein remains largely uncharacterized. The spectrum of disease causing mutations identified so far include missense mutations within the catalytic domain, deletions, insertions, or nonsense mutations causing the premature termination of the protein distributed in the entire open reading frame, and, finally, deletions of genomic regions including the entire *CDKL5* locus. Attempts to draw a correlation between mutation type and disease severity are still hampered by the rather few patients with mutations in CDKL5 and the limited knowledge of its role in the nervous system and how its activities are regulated. The establishment of a genotype-phenotype correlation necessitates therefore that we gain more insight into the neuronal functions of CDKL5.

In this study we examined the expression pattern of the CDKL5 protein in the developing mouse brain and compared it to that of MeCP2, which is the only known substrate of the kinase identified so far (11, 29). Previous *in situ* hybridization

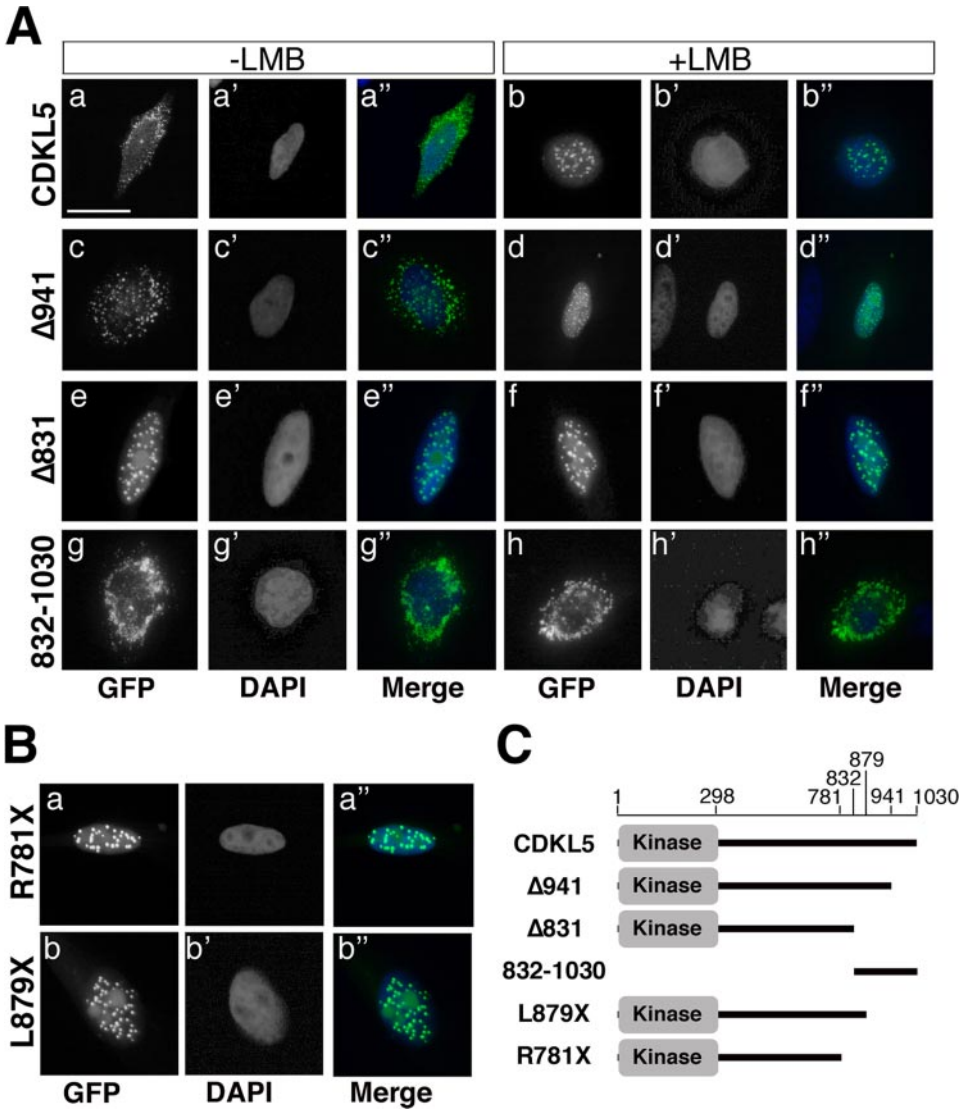

FIGURE 7. **The C-terminal region mediates LMB-sensitive cytoplasmic localization of CDKL5.** *A*, CDKL5, or the indicated derivatives, were fused to GFP, transiently overexpressed in human HeLa cells, and the subcellular localization analyzed 16 h after transfection. *Right panels* show the subcellular distribution in cells treated with 50 mM LMB for 3 h. DAPI was used to stain the nuclei of fixed cells. *B*, two CDKL5 derivatives carrying RTT causing truncating mutations were fused to GFP and their subcellular localization analyzed in HeLa cells. *C*, schematic illustration of the CDKL5 derivatives used in the above experiments. All derivatives carried GFP in the N terminus. *Scale bar* = 10 μm.

experiments revealed that the two genes have partially overlapping expression patterns that are simultaneous activated during development (11). Our studies, based on a polyclonal anti-CDKL5 antibody purified against the antigen confirm these data but provide a more detailed comprehension of the temporal and spatial expression pattern of the two proteins. At the regional level, we detected both proteins in all the main brain areas of adult mice by immunohistochemistry and Western blotting in accordance with the hypothesis that they act in a common molecular pathway. However, the two proteins seem to differ with respect to onset of expression as well as their relative abundance. In fact, MeCP2 is induced during embryogenesis and its levels remain rather constant during postnatal stages until adulthood. CDKL5 levels, on the other hand, are very low in the embryonic brain and are strongly induced during the first two postnatal weeks in accordance with a possible role of the protein in neuronal maturation as in the case of MeCP2. Moreover, CDKL5 levels also vary significantly at the regional level in the brain of adult mice. The highest levels were observed in cortex, hippocampus, and striatum whereas very low levels were found in the cerebellum, which on the other hand is characterized by high levels of MeCP2. It is interesting to note, though, that MeCP2 levels increase significantly in the cerebellum concomitantly with CDKL5 induction. The apparent difference in the modulation of CDKL5 and MeCP2 levels probably reflects the distinct functions of the two proteins, one being a kinase and the other a chromatin-binding protein. At the cellular level, we could detect CDKL5 in all mature NeuN-positive neurons. In cultured primary neurons we detected CDKL5 in glutamatergic as well as GABAergic neurons (data not shown). In the adult mouse brain, however, we observed that GABAergic neurons in the hippocampus and also Purkinje cells seem to express higher levels of CDKL5 raising the possibility that the kinase plays a specific role in this neuronal subtype. The only cells in which we noted a significant difference in CDKL5 and MeCP2 expression were cultured astrocytes; in fact, whereas CDKL5 was virtually undetectable, we could detect low but significant levels of MeCP2 in accordance with a recent publication (36).

Our immunofluorescence experiments on cultured cortical neurons showed that CDKL5 is localized in both of the two main cellular compartments. Interestingly, cytoplasmic CDKL5 appears in the dendritic branches with a distinct punctuate staining. The dendritic localization of the kinase is in accordance with the overlap between CDKL5- and MAP2-positive branches in the striatum of the adult mouse brain and raises the possibility that CDKL5 might be involved in transmitting signals from the synaptic branches to the cell nucleus or *vice versa*. An interesting feature of CDKL5 that distinguishes it from MeCP2 is the modulation of its subcellular distribution at the regional and temporal level. By Western blotting we observed an almost even distribution of CDKL5 between the nucleus and cytoplasm in cortex, hypothalamus, and thalamus, whereas a cytoplasmic accumulation was detected in cerebellum and striatum. It is noteworthy that CDKL5 seems to be excluded from the cell nucleus at the initial

stages of expression and becomes nuclear only during early postnatal stages concomitantly with the strong induction of expression correlating with neuronal maturation. We suspect that CDKL5 exerts its most relevant functions in the cell nucleus and that its localization in this cell compartment is tightly regulated. This seems to be supported by the distribution of the protein in the cerebellum where its abundance is very low and its localization mainly restricted to the cytoplasm.

The spatial and temporal variation in the ratio between nuclear and cytoplasmic CDKL5 suggests that its functions might be modulated through mechanisms regulating its subcellular localization. In accordance with this we show that the C-terminal region of human CDKL5 is important for localizing the protein properly in overexpressing cells. In fact, a GFP-CDKL5 fusion protein was localized in both the cytoplasm and the nucleus in most HeLa cells expressing the protein, whereas a truncated protein, GFP-Δ831, was almost entirely nuclear in all cells. Moreover, the partial cytoplasmic localization of the full-length protein depends on nuclear export mediated by the CRM1 nuclear export receptor, illustrated by the accumulation of GFP-CDKL5 into the nucleus of cells treated with the CRM1 inhibitor LMB. Whether this is due to a direct interaction between CDKL5 and CRM1 or an indirect mechanism is not clear yet. The C-terminal region, required for the cytoplasmic localization of CDKL5, contains a leucine-rich sequence, positioned at 836–845, resembling the consensus NES shown to be the target of CRM1; however, this signal alone is not sufficient for driving a heterologous protein, GFP, to the cytoplasm, and, moreover, the mutagenesis of three leucines into alanines did not alter the subcellular localization of the protein suggesting that other signals might be involved. Moreover, the dynamics of the nuclear accumulation of CDKL5 upon LMB treatment is rather slow raising the possibility that an indirect mechanism might be responsible for driving the kinase out of the nucleus.

The entry of CDKL5 into the nucleus probably depends on two NLS-like stretches of basic amino acids within the long tail of the protein. The most N-terminal NLS, from 312–315, seems to be sufficient for driving the CDKL5 R781X derivative to the nucleus and the more C-terminal, located at 784–789, is sufficient for nuclear import of a GFP fusion protein (data not shown). Eventually, our previous results and data not shown clearly indicate a role of the catalytic activity of CDKL5 for its nuclear accumulation (29).

Considering all above, we suggest that the actual localization of CDKL5 in a given cell depends on the balance between nuclear import and export, direct or indirect, of the protein. We are inclined toward a model where CDKL5 enzymatic activity and the C-terminal tail are necessary to finely tune its dynamic subcellular distribution. Even though future experiments will lead to a detailed molecular model, we propose that the conformation of CDKL5 as well as its interaction with other proteins both modulated by phosphorylation, are involved. We believe that also the physiological state of the cell is important for determining the final outcome. Accordingly, as mentioned above, our immunofluorescence experiments demonstrate that even though most of GFP-CDKL5 was contained in both compartments, some cells were characterized by an either exclusively nuclear or cytoplasmic staining. We believe that various signaling mechanisms, which are still unknown, are involved in modulating the accessibility of CDKL5 to its substrates and that the disruption of this regulation might be detrimental for neuronal function. Besides MeCP2, no substrates of CDKL5 have been identified and only future experiments will reveal whether the kinase has targets also in the cytoplasm (11, 29).

In this work, we have demonstrated a role of the C-terminal region of CDKL5 in regulating the shuttling of the protein between the nucleus and the cytoplasm. Previously, the C terminus has been shown to influence negatively the catalytic activity of CDKL5 (29, 40). Altogether, it appears that this region exerts multiple regulatory functions on the protein in accordance with the fact that disease-causing mutations truncating the protein prematurely have severe consequences for neuronal functions. The two RTT CDKL5 derivatives that we have analyzed, R781X and L879X, are both mislocalized to the cell nucleus and are both characterized by an increase in autocatalytic activity (29).[4] We therefore suggest that their constitutive localization and the increased kinase activity might make them behave as gain of function mutations. Even if attempts to draw a genotype-phenotype correlation have not been able to give clear results, it has recently been suggested that missense mutations negatively affecting the catalytic activity of CDKL5 are associated with a more severe clinical picture than that caused by late truncating mutations (10, 39). Based on our results we therefore propose that the absence or reduction of CDKL5 kinase functions have a greater impact on the nervous system than a gain of activity.

Acknowledgments—We thank the ProRETT Ricerca Parents Association for supporting this research and members of the laboratory for constructive comments.

REFERENCES

1. Hagberg, B., Aicardi, J., Dias, K., and Ramos, O. (1983) *Ann. Neurol.* **14,** 471–479
2. Hagberg, B., Goutieres, F., Hanefeld, F., Rett, A., and Wilson, J. (1985) *Brain Dev.* **7,** 372–373
3. Armstrong, D. D. (2002) *Ment. Retard. Dev. Disabil. Res. Rev.* **8,** 72–76
4. Hagberg, B. A., and Skjeldal, O. H. (1994) *Pediatr. Neurol.* **11,** 5–11
5. Amir, R. E. (1999) *Nat. Genet.* **23,** 185–188
6. Wan, M., Lee, S. S., Zhang, X., Houwink-Manville, I., Song, H. R., Amir, R. E., Budden, S., Naidu, S., Pereira, J. L., Lo, I. F., Zoghbi, H. Y., Schanen, N. C., and Francke, U. (1999) *Am. J. Hum. Genet.* **65,** 1520–1529
7. Tao, J., Van Esch, H., Hagedorn-Greiwe, M., Hoffmann, K., Moser, B., Raynaud, M., Sperner, J., Fryns, J. P., Schwinger, E., Gécz, J., *et al.* (2004) *Am. J. Hum. Genet.* **75,** 1149–1154
8. Weaving, L. S., Christodoulou, J., Williamson, S. L., Friend, K. L., McKenzie, O. L. D., Archer, H., Evans, J., Clarke, A., Pelka, G. J., Tam, P. P. L., *et al.* (2004) *Am. J. Hum. Genet.* **75,** 1079–1093
9. Scala, E., Ariani, F., Mari, F., Caselli, R., Pescucci, C., Longo, I., Meloni, I., Giachino, D., Bruttini, M., Hayek, G., *et al.* (2005) *J. Med. Genet.* **42,** 103–107
10. Evans, J. C., Archer, H. L., Colley, J. P., Ravn, K., Nielsen, J. B., Kerr, A., Williams, E., Christodoulou, J., Gecz, J., Jardine, P. E., Wright, M. J., Pilz, D. T., Lazarou, L., Cooper, D. N., Sampson, J. R., Butler, R., Whatley, S. D., and Clarke, A. J. (2005) *Eur. J. Hum. Genet.* **13,** 1113–1120
11. Mari, F., Azimonti, S., Bertani, I., Bolognese, F., Colombo, E., Caselli, R., Scala, E., Longo, I., Grosso, S., Pescucci, C., Ariani, F., Hayek, G., Balestri,

[4] N. Landsberger, unpublished results.

P., Bergo, A., Badaracco, G., Zappella, M., Broccoli, V., Renieri, A., Kilstrup-Nielsen, C., and Landsberger, N. (2005) *Hum. Mol. Genet.* **14,** 1935–1946
12. Cheadle, J. P., Gill, H., Fleming, N., Maynard, J., Kerr, A., Leonard, H., Krawczak, M., Cooper, D. N., Lynch, S., Thomas, N., Hughes, H., Hulten, M., Ravine, D., Sampson, J. R., and Clarke, A. (2000) *Hum. Mol. Genet.* **9,** 1119–1129
13. Hanefeld, F. (1985) *Brain Dev.* **7,** 320–325
14. Kalscheuer, V. M., Tao, J., Donnelly, A., Hollway, G., Schwinger, E., Kubart, S., Menzel, C., Hoeltzenbein, M., Tommerup, N., Eyre, H., Harbord, M., Haan, E., Sutherland, G. R., Ropers, H. H., and Gécz, J. (2003) *Am. J. Hum. Genet.* **72,** 1401–1411
15. Archer, H. L., Evans, J., Edwards, S., Colley, J., Newbury-Ecob, R., O'Callaghan, F., Huyton, M., O'Regan, M., Tolmie, J., Sampson, J., Clarke, A., and Osborne, J. (2006). *J. Med. Genet.* **43,** 729–734
16. Van Esch, H., Jansen, A., Bauters, M., Froyen, G., and Fryns, J. P. (2007) *Am. J. Med. Genet. A.* **143,** 364–369
17. Jones, P. L., Veenstra, G. J., Wade, P. A., Vermaak, D., Kass, S. U., Landsberger, N., Strouboulis, J., and Wolffe, A. P. (1998) *Nat. Genet.* **19,** 187–191
18. Nan, X., Ng, H. H., Johnson, C. A., Laherty, C. D., Turner, B. M., Eisenman, R. N., and Bird, A. (1998) *Nature* **393,** 386–389
19. Fuks, F., Hurd, P. J., Wolf, D., Nan, X., Bird, A. P., and Kouzarides, T. (2002) *J. Biol. Chem.* **278,** 4035–4040
20. Chahrour, M., and Zoghbi, H. Y. (2007) *Neuron* **56,** 422–437
21. Chen, W. G., Chang, Q., Lin, X., Meissner, A., West, A. E., Griffith, E. C., Janisch, R., and Greenberg, M. E. (2003) *Science* **302,** 885–889
22. Martinowich, K., Hattori, D., Wu, H., Fouse, S., He, F., Hu, Y., Fan, G., and Sun, Y. E. (2003) *Science* **302,** 890–893
23. Zhou, Z., Hong, E. J., Cohen, S., Zhao, W. N., Ho, H. Y., Schmidt, L., Chen, W. G., Lin, Y., Savner, E., Griffith, E. C., Hu, L., Steen, J. A., Weitz, C. J., and Greenberg, M. E. (2006) *Neuron* **52,** 255–269
24. Young, J. I., Hong, E. P., Castle, J. C., Crespo-Barreto, J., Bowman, A. B., Rose, M. F., Kang, D., Richman, R., Johnson, J. M., Berget, S., and Zoghbi, H. Y. (2005). *Proc. Natl. Acad. Sci. U. S. A.* **102,** 17551–17558
25. Yasui, D. H., Sailaja, P., Bieda, M. C., Vallero, R. O., Hogart, A., Nagarajan, R. P., Thatcher, K. N., Farnham, P. J., and LaSalle, J. M. (2007). *Proc. Natl. Acad. Sci. U. S. A.* **104,** 19416–19421
26. Ishibashi, T., Thambirajah, A. A., and Ausiò, T. J. (2008) *FEBS Lett.* **582,** 1157–1162
27. Chahrour, M., Jung, S. Y., Shaw, C., Zhou, X., Wong, S. T., Qin, J., and Zoghbi, H. Y. (2008) *Science* **320,** 1224–1229
28. Montini, E., Andolfi, G., Caruso, A., Brchner, G., Walpole, S. M., Mariani, M., Consalez, G., Trump, D., Ballabio, A., and Franco, B. (1998) *Genomics* **51,** 427–433
29. Bertani, I., Rusconi, L., Bolognese, F., Forlani, G., Conca, B., De Monte, L., Badaracco, G., Landsberger, N., and Kilstrup-Nielsen, C. (2006) *J. Biol. Chem.* **281,** 32048–32056
30. Rosas-Vargas, H., Bahi-Buisson, N., Philippe, C., Nectoux, J., Girard, B., N'Guyen Morel, M. A., Gitaux, C., Lazzaro, L., Odent, S., Jonveaux, P., Chelly, J., and Bienvenu, T. (2007) *J. Med. Genet.* **45,** 172–178
31. Shahbazian, M. D., Antalffy, B., Armstrong, D. L., and Zoghbi, H. Y. (2002) *Hum. Mol. Genet.* **11,** 115–124
32. Jung, B., Jugloff, D. G. M., Zhang, G., Logan, R., Brown, S., and Eubanks, J. H. (2002) *J. Neurobiol.* **55,** 86–96
33. Mullaney, B. C., Johnston, M. V., and Blue, M. E. (2004) *Neuroscience* **123,** 939–949
34. Kishi, N., and Macklis, J. D. (2004) *Mol. Cell. Neurosci.* **27,** 306–321
35. Kaufmann, W. E., Johnston, M. V., and Blue, M. E. (2005) *Brain Dev.* **27,** S77–S87
36. Schmid, R. S., Tsujimoto, N., Qu, Q., Lei, H., Li, E., Chen, T., and Blaustein, C. S. (2007) *Neuroreport* **19,** 393–398
37. Fornerod, M., Ohno, M., Yoshida, M., and Mattaj, I. W. (1997) *Cell* **90,** 1051–1060
38. La Cour, T., Kiemer, L., Mølgaard, A., Gupta, R., Skriver, K., and Brunak, S. (2004) *Protein Eng. Des. Sel.* **17,** 527–536
39. Bahi-Buisson, N., Kaminska, A., Boddaert, N., Rio, M., Afenjar, A., Gèerard, M., Giuliano, F., Motte, J., Hèron, D., Morel, M. A., Plouin, P., Richelme, C., des Portes, V., Dulac, O., Philippe, C., Chiron, C., Nabbout, R., and Bienvenu, T. (2008) *Epilepsia* **49,** 1027–1037
40. Lin, C., Franco, B., and Rosner, M. R. (2005) *Hum. Mol. Genet.* **14,** 3775–3786